Design and Fabrication of a Surface-Wave Accelerator Based on Silicon Carbide

Gennady Shvets and Sergey Kalmykov

Citation: AIP Conference Proceedings **737**, 983 (2004); doi: 10.1063/1.1842652

View online: http://dx.doi.org/10.1063/1.1842652

View Table of Contents: http://scitation.aip.org/content/aip/proceeding/aipcp/737?ver=pdfcov

Published by the AIP Publishing

Design and Fabrication of a Surface-Wave Accelerator Based on Silicon Carbide

Gennady Shvets and Sergey Kalmykov

Department of Physics and Institute for Fusion Studies, The University of Texas at Austin, Austin, TX 78712

Abstract. The principles and electromagnetic simulations of a novel accelerating structure are described. The structure is planar, consisting of two plates of silicon carbide (SiC) separated by a vacuum gap. Charged particle bunches are accelerated in the vacuum gap by the surface electromagnetic waves (phonon polaritons) localized near the vacuum/SiC interface. The structure can be powered by a carbon dioxide (CO_2) laser with the wavelength $\lambda_0 \approx 10.6\mu$m. The operating wavelength is dictated by the frequency-dependent dielectric permittivity $\varepsilon(\omega)$ of SiC which is negative for the frequencies in the CO_2 tunability range. The resulting accelerator can support accelerating fields well in excess of 1 GeV/m without breakdown, and provide the path to compact and inexpensive particle accelerators. The challenge of coupling radiation into a very narrow (a few microns) vacuum gap is resolved by designing a coupling grating on the top surface of a Si wafer, and attaching a thin SiC film to the bottom of the wafer. Preliminary fabrication results are reported.

1. INTRODUCTION

Laser-driven accelerators of charged particles hold the promise of extremely high accelerating gradients and, therefore, significant reduction of the acceleration length. Because the electric field of a laser is essentially transverse, in order to impart energy to a charged particle, it has to be rotated using an accelerating structure. Examples of such structures include an open grating in an inverse Smith-Purcell accelerator [1], a dielectric-loaded accelerator [2, 3], an overmoded micro-channel metal waveguide [4], or a photonic bandgap accelerator [5, 6, 7].

All these schemes have important limitations. For example, the Inverse Smith-Purcell Accelerator with the grating grooves along y direction is unsuitable for relativistic particle acceleration if the incident laser beam is in the $x-z$ plane because the resulting luminous wave is transversely polarized. Obliquely incident laser beam (with a non-vanishing k_y wavenumber component) has a finite magnetic field normal to the grating surface which deflects the electron beam. The dielectric-loaded accelerator needs a metallic casing to confine radiation. Metals are lossy at infrared frequencies and susceptible to breakdown for high field amplitudes. Because the electric field at the metallic wall is of the same order as the peak accelerating field in the vacuum gap, breakdown and pulsed heating of the metallic casing is a serious issue. The overmoded micro-channel metal waveguide suffers from the same limitation as the dielectric accelerator (metal at high field), and, in addition, has a low shunt impedance because the electric field in an overmoded guide is primarily transverse. It is the purpose of this work to introduce an accelerating structure which does not suffer from the above limitations. It has no

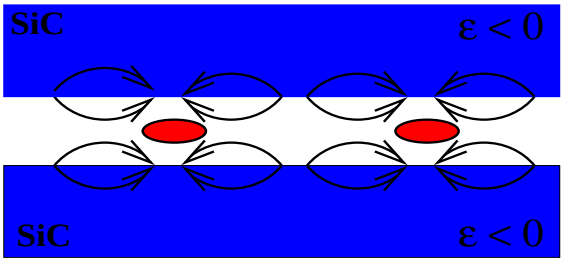

FIGURE 1. Schematic of the Surface Wave Accelerator Based on SiC (SWABSiC). Acceleration takes place inside the vacuum gap between two parallel plates made of silicon carbide. Field lines extend from the surface of the SiC/vacuum interface into the channel and accelerate particle bunches (two bunches spaced by one acceleration wavelength are shown). Surface waves are localized near vacuum/SiC interfaces.

metallic parts and has a narrow accelerating gap (to maximize $E_x/E_\perp$, where E_x is the accelerating field component).

We refer to this accelerating structure as the Surface Wave Accelerator Based on SiC (SWABSiC) because the accelerating waves are the surface phonon polaritons confined to the vacuum/SiC interface. A rough schematic of the device is shown in Fig. 1. It is well known that surface waves can only exist at the interface of the two media with opposing signs of the dielectric permittivity ε. It turns out that SiC does indeed have $\varepsilon < 0$ for $\lambda = 10.6\mu$m which is the wavelength of the CO_2 laser. The normal component of the electric field $E_\perp$ changes sign at the vacuum/SiC interface (see Fig. 1) to ensure the continuity of $\varepsilon E_\perp$ across the interface. To minimize the $E_\perp/E_x$ ratio, the gap size between SiC films has to be small, typically $\sim \lambda/3 \approx 3\mu$m. Thus, one of the major practical problems with SWABSiC is coupling radiation into such a small opening. This problem is further exacerbated by the small group velocity of the accelerating wave: even if radiation can be coupled into the opening hole of the structure, it is likely to get attenuated after propagating through the entire accelerator length. The coupling problem is resolved by making a significant modification to the conceptual schematic shown in Fig. 1 as described in Section 3.

The rest of the paper is organized as follows. In Sec. 2 basic material properties of SiC are reviewed, and the electromagnetic (EM) properties of the simplified SiC accelerating structure shown in Fig. (1) are described. A more realistic and amenable to effective laser coupling structure shown in Fig. 3 is introduced in Section 3, and the supporting numerical simulations of laser coupling into the structure are described. Preliminary progress on fabricating the SWABSiC accelerator using conventional microfabrication techniques are reported in Sec. 4.

2. DESCRIPTION OF SIC AND EM PROPERTIES OF THE CONCEPTUAL ACCELERATING STRUCTURE

Silicon carbide (SiC) is a hard crystalline material which comes in a variety of polytypes. We concentrate only on the cubic 3C-SiC polytype which can be grown on Si wafers. SiC is a wide bandgap ($V = 2.3$ V) semiconductor. Because of the wide bandgap, SiC exhibits a very high electrical breakdown field (300 MV/m DC). Silicon carbide is presently used for advanced semiconductor electronic device applications. SiC-based electronics and sensors can operate in hostile environments (600 C = 1112 F) where conventional silicon-based electronics (limited to 350 C) cannot function. Silicon carbide's ability to function in high temperature, high power, and high radiation conditions are equally important for the field of accelerator physics. This is because future accelerators must operate at high accelerating gradients (large electric and magnetic fields), withstand significant heating due to the ohmic dissipation of the accelerating fields, and tolerate occasional beam loss and radiation by the accelerating particles executing transverse (betatron) oscillations. Equally important is the high thermal conductivity, $\approx 3.8 W/cm/K$.

Another important feature of SiC is that its frequency-dependent dielectric permittivity is negative in a narrow frequency band $\omega_T < \omega < \omega_L$ [8]:

$$\varepsilon_c(\omega) = \varepsilon_\infty \frac{\omega_L^2 - \omega^2 - i\gamma\omega}{\omega_T^2 - \omega^2 - i\gamma\omega}, \tag{1}$$

where $\omega_L = 972\text{cm}^{-1}$ ($\lambda_L = 1/\omega_L = 10.29\mu\text{m}$) and $\omega_T = 796\text{cm}^{-1}$ ($\lambda_T = 1/\omega_T = 12.56\mu\text{m}$) are the frequencies of the longitudinal and transverse optical phonons, respectively. The damping constant $\gamma = 5\text{cm}^{-1}$ is relatively small and can be neglected in analytic calculations. Of course, losses are fully accounted for in our numerical simulations. The high-frequency dielectric constant $\varepsilon_\infty = 6.5$ for the 3C-SiC crystal. Frequency dependence of the dielectric permittivity given by Eq. (1) is characteristic of ionic crystals, of which SiC is one example. There are, however, many other ionic crystals with different characteristic frequencies ω_L and ω_T. They can be also be potentially used as the material for accelerator walls. It is important that the dielectric permittivity $\varepsilon(\omega)$ of SiC is negative at $\lambda = 10.6\mu\text{m}$ produced by a CO_2 laser. Thus, there is a natural widely available power source for the SiC-based accelerating structures.

The conceptual accelerating structure (CAS) is shown in Fig. (1). Acceleration takes place in the vacuum gap between two parallel SiC plates. Accelerating field is generated by the surface charges at the SiC/vacuum interface. Because of the negative dielectric permittivity of SiC, the electromagnetic wave exponentially decays inside the confining SiC walls. Therefore, unlike the standard planar dielectric accelerator, the proposed SiC accelerator does not require a metal casing.

Below we consider EM properties of the accelerating (fundamental) mode of the CAS. This mode has the maximum of the accelerating field on axis, and its deflecting electric and magnetic fields vanish on axis. Assume that thick SiC plates forming the cladding of the waveguide are separated by the distance $2b$ in y-direction, and are infinite in the $x-z$ plane. Vacuum-SiC interfaces are assumed at $y = \pm b$. Consider the mode accelerating particles in x-direction that has non-vanishing field components E_x, E_y, and B_z. The

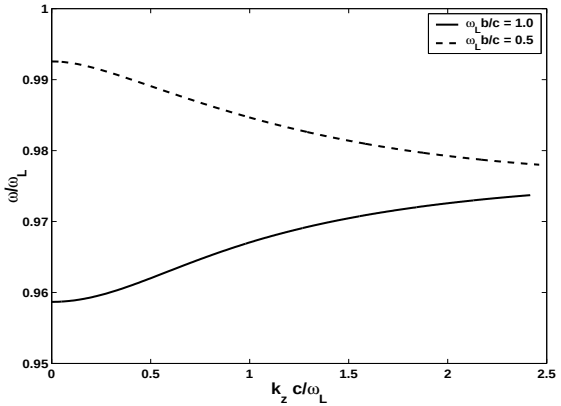

FIGURE 2. Dispersion for two separations between SiC plates, $\omega_L b/c = 1.0$ (positive group velocity) and $\omega_L b/c = 0.5$ (negative group velocity).

accelerating field E_x is assumed symmetric while B_z and E_y anti-symmetric with respect to the $y = 0$ centerplane. All three field components are assumed to have the dependence $\exp i(k_x x - \omega t)$. Magnetic field B_z is given by

$$B_z = \frac{\sin \chi_v y}{\sin \chi_v b} \quad \text{for} \quad |y| < b, \quad \text{and} \quad B_z = e^{-\chi_c(|y|-b)} \quad \text{for} \quad |y| > b, \tag{2}$$

where $\chi_v^2 = \omega^2/c^2 - k_x^2$ and $\chi_c^2 = -\omega^2\varepsilon_c/c^2 + k_x^2$. Electric field components are expressed through B_z: $E_x = (ic/\varepsilon\omega)\partial_y B_z$ and $E_z = (k_x c/\varepsilon\omega)B_z$, where $\varepsilon = 1$ in the vacuum gap and $\varepsilon = \varepsilon_c$ inside the SiC cladding.

The dispersion relation ω v. s k_x are shown in Fig. 2, where the wave damping was neglected by setting $\gamma = 0$. Clearly, the group velocity of the wave $v_{\rm gr} = \partial\omega/\partial k_x$ can be either positive or negative, depending on the channel width. Generally, wider channels support waves with positive group velocity and narrower channel support those with negative group velocity. The important thing to notice is that whether the group velocity is negative or positive, it it very small for small gaps between SiC slabs ($v_g/c \sim 0.01$). Because we require that $b \ll \lambda$ to ensure that $E_x \gg E_y$, damping is likely to prevent accelerating wave propagation from $x = 0$ (in-coupling port for CO_2 laser radiation) to $x = L$ (end of the structure). Therefore, a different coupling scheme needs to be implemented. Radiation can be coupled from the top of the structure through a diffractive grating. The necessity to implement the grating coupling renders the CAS obsolete. It is replaced by the SiC-on-Si structure shown in Fig. 3.

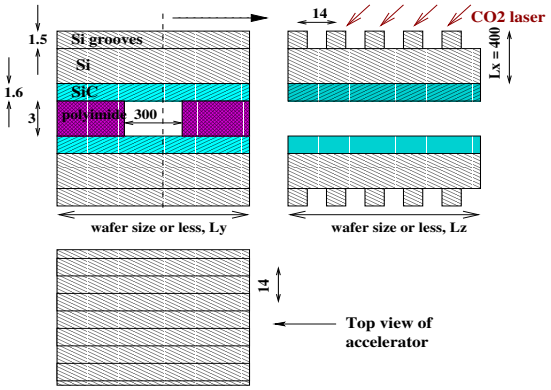

FIGURE 3. Schematic of a realistic surface wave accelerator based on SiC. A thin SiC film is grown on a Si handle wafer. Grating on the wafer is for coupling the laser from vacuum into the wafer. Incident from Si onto SiC radiation couples into the vacuum gap between the SiC films. The two wafers are shown bonded by an organic glue (polyimide). All sizes are given in microns, and are not optimized.

3. SIC ON SI ACCELERATING STRUCTURE

Thin films (between 200nm and several μm) of SiC can be epitaxially grown on Si wafers using atmospheric pressure chemical vapor deposition (APCVD) [9]. A a finite thickness SiC film cannot spatially confine the accelerating mode described in Sec. 2 for indefinite time. In fact, indefinite confinement is not necessary because dissipative losses (finite phonon lifetime due to lattice anharmonicities) limit the mode's lifetime. A thin-film SiC waveguide is a leaky waveguide. Its leakage rate is controlled by the thickness of the SiC film, and has to be chosen not to exceed the dissipative loss rate in order to keep the quality factor of the accelerating mode high. Because radiation can couple out of the structure, it can also couple in from the outside. This enables powering the accelerating mode by a laser pulse incident from outside of the structure. Because using a free-standing several-micron thick film as an accelerating structure is impractical from thermal and mechanical points of view, we have chosen to use thin SiC films attached to a standard (400μm thick) double-polished Si wafer. Fortunately, Si has no infrared resonances and does not introduce any additional damping at $\lambda = 10.6\mu$m. In mid-IR the dielectric permittivity of Si is almost frequency-independent and equal to $\varepsilon_{\rm Si} = 12$.

The schematic of a SiC-on-Si surface wave accelerator is shown in Fig. 3. All dimensions are given in microns and are still tentative. Creating a symmetric accelerating structure requires bonding two Si wafers. One approach is to use an organic glue as shown in Fig. 3. Other approaches are also being considered. Because we are interested in exciting surface waves with $k_x = \omega/c$ capable of accelerating relativistic particles, it is necessary to employ a dielectric grating on the top surface of the Si wafer. To see why, consider a laser beam incident on a smooth (no grating) structure. It excites a surface wave with $k_x = \sin\theta\,\omega/c$, where θ is the incidence angle measured from the wafer normal. This surface wave is unsuitable for continuous particle acceleration because its

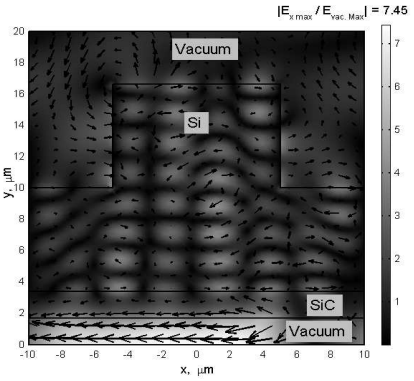

FIGURE 4. Electric field distribution in the accelerating structure driven by a laser beam with $\lambda_0 = 10.685\ \mu$m incident at $\theta = 28^\circ$ angle. Grayscale: $|E_x(x,y)|$ normalized to the incident electric field; arrows - electric field direction and scaled amplitude. Structure parameters: grating depth 13.2μm; SiC thickness 1.7μm; gap width 3.4μm. Phase velocity of the $n = 1$ diffraction order: $v_{ph}/c = 1.00175$.

phase velocity exceeds the speed of light. When the same laser pulse excites a corrugated Si surface, radiation is refracted into Si into several diffraction orders. The corresponding wavenumbers are $k_n = \sin\theta\,\omega/c + 2\pi n/\lambda_g$, where n is the diffractive order and λ_g is the grating periodicity. Luminous wave is excited for the incidence angle $\theta_{\rm lum}$ calculated from $\sin(\theta_{\rm lum}) = 1 - n\lambda/\lambda_g$. For example, by choosing $\lambda_g = 21.2\mu$m and $\lambda = 10.6\mu$m one can excite a luminous mode in the first diffraction order. Several diffraction orders can propagate in Si because of its high dielectric permittivity.

The electromagnetic performance of the SiC-on-Si surface wave accelerator was modelled using a finite elements electromagnetic code FEMLAB. Frequency-dependent $\varepsilon(\omega)$ given by Eq. (1) was assumed (including losses), and $\varepsilon_{\rm Si} = 12$. The results are shown in Fig. 4, where the arrows point in the direction of the electric field. The structure was excited by a laser beam incident at an angle $\theta = 28^\circ$. Note that the electric field on axis is almost entirely longitudinal, and is 7.45 higher than that of the incident laser beam. Hence, the accelerating structure acts as a resonator. The incident wavelength $\lambda_0 = 10.685\ \mu$m was chosen to maximize the total electric field energy in the acceleration region.

Several diffraction orders (and, therefore, several k_n's) are excited in the structure. Only the one with the phase velocity approaching the speed of light is useful for particle acceleration. The depth and period of the grating were chosen such as to optimize the excitation of $k_1 \approx \omega_0/c$ (where $\omega_0 = 2\pi c/\lambda_0$). The normalized on-axis amplitude of the electric field is plotted in Fig. 5(a), and the relative intensities of different diffractive orders n are plotted in Fig 5(b). Clearly, the luminous $n = 1$ mode dominates. This explains why the electric field is essentially longitudinal near the axis: the parasitic (non-luminous) waves which carry significant transverse fields are only weakly excited. In non-optimized runs we observed significant excitation of the parasitic diffraction orders and significant transverse electric field near the axis. The negative diffraction orders

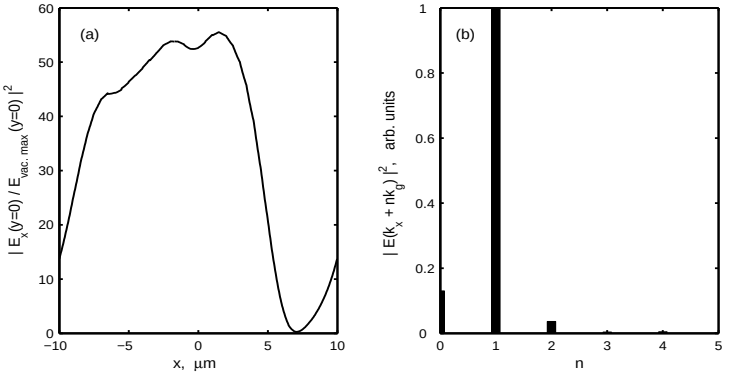

FIGURE 5. (a) Electric field on axis $|E_x(x,0)|$ normalized by the incident laser field at the exact resonance $\lambda_0 = 10.685$ μm; (b) distribution of the integrated on-axis electric field energy v. s. the diffraction order n: $k_n = \sin\theta\,\omega/c + 2\pi n/\lambda_g$. Structure parameters: same as in Fig. 4.

$n = -1, -2, \ldots$ are weakly excited and are not shown in Fig 5(b).

To confirm that the response of the structure is indeed resonant, we have scanned the frequency of the incident laser while keeping the incidence angle fixed at $\theta = 28^\circ$. The total energy U_{gap} contained in the vacuum gap (normalized to what it would have been in the absence of the accelerating structure) is plotted in Fig. 6 as the function of the incident wavelength λ_0. The high sensitivity of U_{gap} to the laser wavelength indicates a resonant excitation of the accelerating mode which can be understood as follows. Whenever the frequency of the incident light $\omega_0 = 2\pi c/\lambda_0$ and the wavenumber of the n-th diffraction order k_n are such that they satisfy the dispersion relation of the surface wave $\omega(k)$ plotted in Fig. 2, the structure is resonantly driven. Because the dispersion curves of the accelerating surface waves are very flat, the sensitivity to the incident wavelength is very strong. On the other hand, the sensitivity to the incidence angle is fairly weak.

4. FABRICATING THE STRUCTURE

We have made some initial progress in fabricating the SiC-on-Si accelerating structure. Using standard microfabrication methods which will be described elsewhere, the accelerating cavity at the bottom of a doubly-polished Si wafer was etched out using selective reactive ion etching (RIE). Cavity dimensions are $2000 \times 400\mu$m, its depth is 2.7μm. The rest of the bottom side was protected by a 1.5μm thick SiO_2 layer. Using the same techniques, we have etched the grating on the top side of the Si wafer. The grating pitch is $\lambda_g = 16\mu$m, its width is 8μm, and its depth is 1.5μm. The total area covered by the grating is a 2×2 mm square. It is located directly above the cavity and entirely covers it.

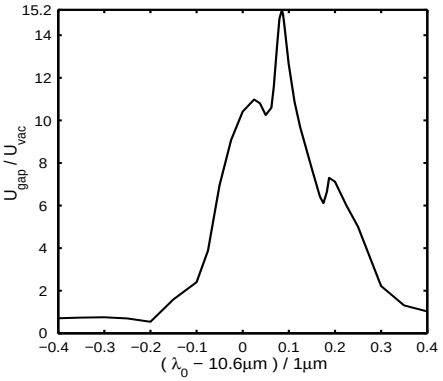

FIGURE 6. Normalized energy in the accelerating gap v. s. laser wavelength. Incidence angle $\theta = 28^\circ$. Structure parameters: same as in Fig. 4.

After the above processing steps the wafer ended up protected by an oxide film everywhere except inside the cavity. It was sent to Case Western Reserve University where a 1.5μm-thick SiC film was grown using APCVD [9]. Crystalline SiC film grows only on Si but not on the amorphous SiO_2. Thus we were able to peel off the amorphous (and weakly adherent) SiC grown on the oxide without damaging the crystalline oxide grown inside the cavity. The wafer was then cleaned from the remaining oxide. The results of the SiC deposition are shown in Fig. 7 (left). Clearly, SiC was deposited only inside the accelerating cavity as desired. The grating area on the top side of the wafer is shown in Fig. 7 (right). The remaining fabrication step involves bonding two identical wafers, and will be described elsewhere.

5. SUMMARY AND FUTURE WORK

The have designed and partially fabricated a novel advanced accelerator: Surface Wave Accelerator Based on SiC (SWABSiC) which can be powered by a pulsed CO_2 laser. The accelerating structure consists of a thin SiC film grown on the bottom of a standard Si wafer. The top side of the wafer has a periodic grating for coupling the laser radiation into the accelerating structure. Numerical simulations of laser coupling into the SWABSiC were carried out, and the accelerating structure was found to be a high-quality resonator. The longitudinal electric field inside the accelerating gap (between two SiC films) was found to be almost an order of magnitude higher than that of the incident laser pulse.

Fabrication of the grating and growth of SiC film have been successfully implemented. Future work will involve aligning and bonding two identical wafers and carrying out the cold tests by measuring the reflection/transmission coefficients of the laser pulse depending on the laser frequency and incidence angle. Future numerical work will

FIGURE 7. Fabrication of the SWABSiC for cold testing (no particles).(Left) Accelerating cavity etched in the lower side of the Si wafer. A 1.5μm film of single-crystalline 3C-SiC was deposited on the inner surface of the cavity using atmospheric pressure chemical vapor deposition. For the real accelerator the cavity will be substituted by a trench to allow particle passage. (Right) A $\lambda_g = 16\mu$m period grating (for laser coupling) was etched on the upper surface of the Si wafer. Grating depth: 1.5μm.

also address the issues of thermal load of the structure.

REFERENCES

1. R. Palmer *et. al.* in *Laser Acceleration of Particles*, edited by C. Joshi and T. Katsouleas, AIP Conf. Proc. 130 (AIP, New York, 1985).
2. J. Rosenzweig, A. Murokh, and C. Pellegrini, Phys. Rev. Lett. **74,** 2467 (1995).
3. A. Tremaine, J. Rosenzweig, and P. Schoessow, Phys. Rev. E **56,** 7204 (1997).
4. L. C. Steinhauer and W. D. Kimura, Phys. Rev. ST-AB **6,** 061302 (2003).
5. D. R. Smith *et. al.,* Appl. Phys. Lett. **65,** 645 (1994).
6. M. A. Shapiro *et. al.* Phys. Rev. ST-AB **4,** 042001 (2001).
7. B. M. Cowan, Phys. Rev. ST-AB **6,** 101301 (2003).
8. A. Shchegrov *et. al.,* Phys. Rev. Lett. **85,** 1548 (2000); W. G. Spitzer, D. Kleinman, and D. Walsh, Phys. Rev. **113,** 127 (1959).
9. C. A. Zorman *et. al.* J. Appl. Phys. **78,** 5136 (1995).

ACKNOWLEDGMENTS

Support for this work was provided by the US Department of Energy under the Contract No. DE-FG02-04ER41321.